



## RESEARCH ARTICLE

### Silver Nanoparticles: Green Synthesis, Characterization, Blood Compatibility and Protoscolicidal Efficacy against *Echinococcus granulosus*

Parwin Jalal Jalil<sup>1</sup>, Bushra Hussain Shnawa<sup>1,2,\*</sup> and Samir Mustafa Hamad<sup>2</sup>

<sup>1</sup>Biology Department, Science Faculty, Soran University, Kurdistan-Iraq

<sup>2</sup>Scientific Research Centre, Soran University, Kurdistan- Iraq

\*Corresponding author: bushra.shnawa@soran.edu.iq

#### ARTICLE HISTORY (21-093)

Received: February 21, 2021  
Revised: April 2, 2021  
Accepted: April 4, 2021  
Published online: April 15, 2021

#### Key words:

*Echinococcus granulosus*  
*Zizyphus spina- christi*  
Silver Nanoparticles  
Protoscolicidal

#### ABSTRACT

Spillage of protoscoleces within hydatid fluid during surgery for hydatid cyst is the main reason for its recurrence. Therefore, to inactivate the protoscoleces, various scolicidal substances have been tested. However, novel and more efficient agents are needed owing to several associated complications. This study focused on the effects of green synthetic Silver Nanoparticles (AgNPs) from *Zizyphus spina-christi* leaves on *Echinococcus granulosus* protoscoleces. Also, to evaluate the blood compatibility of Ag NPs. The Ag NPs were identified by ultraviolet-visible (UV-Visible) spectrophotometer, X-ray diffraction (XRD), Scanning electron microscopy imaging, and Energy-dispersive X-ray spectroscopy (EDX). Hydatid fluid was aspirated aseptically from cysts of infected sheep liver. The protoscoleces were exposed to Ag NPs at several concentrations. Also, scanning electron microscopy for ultrastructural changes and *in vitro* erythrocytes lysis was performed. The Ag NPs were spherical; the particles' size reached 50 nm, and presented a surface plasmon peak around 460 nm. The current study's findings indicated the powerful *in vitro* scolicidal efficacy of the green biosynthesized AgNPs. Several morphological alterations were observed on the protoscoleces by optical and scanning electron microscopy. Lysis of RBCs at different doses of Ag NPs was significantly ( $P \leq 0.05$ ) less than the positive control value, thus proposing its biocompatibility. This work suggests that chemicals like polyphenols present in the extract of *Z. spina-christi* act as reducing and stabilizers agents to create Ag NPs. Nevertheless, further investigations are needed to investigate the Ag NPs scolicidal effects in animal models.

©2021 PVJ. All rights reserved

**To Cite This Article:** Jalil PJ, Shnawa BH, and Hamad SM, 2021. Silver nanoparticles: green synthesis, characterization, blood compatibility, and protoscolicidal efficacy against *Echinococcus granulosus*. Pak Vet J, 41(3): 393-399. <http://dx.doi.org/10.29261/pakvetj/2021.039>

#### INTRODUCTION

Cystic echinococcosis (CE) is a worldwide distributed parasitic disease resulted from the hydatid cyst of *Echinococcus granulosus*. It is also described as a zoonotic disease referred to as hydatid disease, or hydatidosis (Kern *et al.*, 2017). The World Health Organization classified it with neglected tropical infections (WHO, 2010). The infection is naturally transmitted between canids as definitive and livestock as intermediate hosts, including humans. The highest prevalence is recorded from sheep-raising areas where many stray dogs exist and consume the infected animals' organs. In Iraq, hydatidosis is considered hyperendemic. It is also one of the countries' significant helminthic

infections with socioeconomic impacts targeting humans and their livestock (Benyan *et al.*, 2013).

However, surgical operation remains the chief therapeutic method; nevertheless, other techniques also have an essential role in CE control. Leakage of cyst fluid is the primary cause for the recurrence of the infection during surgery. Therefore, killing the protoscoleces within the cyst during the surgical procedure is essential. All of the scolicidal agents have adverse effects (Shi *et al.*, 2016). For instance, the WHO recommended Benzimidazole as a medication for human infection. This drug is known to possess parasitostatic rather than parasiticidal effects. Low water solubility and low absorption of Benzimidazole may be responsible for its treatment failure. Also, it has many severe side effects on

CE patients' life-span and prognosis. These facts underline the need for new drugs (Siles-Lucas *et al.*, 2018). Therefore, researchers have achieved several attempts to increase the compound's solubility, absorption, and bioavailability. Among these trials that improved the drug efficiency is the addition of NPs, which results in increasing the intra-cystic permeability for the curing compound (Siles-Lucas *et al.*, 2018). Recently, Shnawa (2018) reviewed many published articles investigating the protoscolicidal impacts of green synthetic NPs against protoscoleces of *E. granulosus*. Two previous researches investigated the green synthesized silver and gold nanoparticles' activity from *Penicillium aculeatum* against the protoscoleces of *E. granulosus*. The authors stated that these NPs could be a potential scolicidal agent for CE therapy (Rahimi *et al.*, 2015; Barabadi *et al.*, 2017). More recently, Salih *et al.* (2020) concluded that the biosynthesized Ag NPs from some plant extracts showed remarkable effects against *E. granulosus*, particularly *Eucalyptus globulus* extract.

The present work aimed to investigate the effect of green synthesis AgNPs by *Z. spina christi* extract against *E. granulosus* protoscoleces and assess the produced nanoparticles' hemolytic ability on human erythrocytes.

## MATERIALS AND METHODS

### Preparation of the *Zizyphus spina - christi* Leaves Extract:

Fresh leaves of the *Z. spina-christi* were brought from Erbil city, Iraq. The plant extracts were prepared by weighing 25 gm of leaves, which were cut into small parts, added to 100 mL of double-distilled water, and heated to 90°C for 40 min. The contents were then filtered and kept at 4°C for nanoparticle synthesis (Halawani, 2017).

**Synthesis and Description of Ag Nanoparticles:** The 10 mL of prepared *Z. spina christi* leaves extract was added to 100 mL silver nitrate (1mM), which was dropped at 80°C for 1 hour until the mixture's color is changed and the production of dark brown precipitation. This indicating the formation of silver nanoparticles. The precipitation was centrifuged at 7000 rpm. Finally, Ag NPs were annealed using a Bunsen burner (Fig. 1).

The morphology of the synthesized Ag NPs was examined by Fast Emission SEM (FE-SEM, Quanta 4500). The optical absorptions of Ag NPs were recorded using double-beam UV-Visible spectra (Super Aquarius spectrophotometer). Also, the chemical composition of the material was measured by EDX. The nanoparticles' crystal arrangement was studied by X-ray diffraction (XRD) by PAN-analytical X' Pert PRO (Cu K $\alpha$  = 1.5406 Å). The scanning rate was 1 °/min in the 2 $\theta$  range from 20° to 80° (Oluwaniyi *et al.*, 2016). All experiments were performed in the scientific research center of Soran University, Iraq.

**Collection of Protoscoleces:** The parasite was collected from hepatic cysts of naturally infected sheep slaughtered at the abattoir in Soran city-Erbil. The protoscoleces were harvested by aspirating the hydatid fluid. The protoscoleces' viability was evaluated by 0.1% eosin dye (Smyth and Barrett, 1980). Colorless protoscoleces were

considered as viable, whereas red-colored protoscoleces were recorded as dead.

### *In vitro* Protoscolicidal Effect of Ag NPs

***In vitro* Protoscolicidal Effect of Ag NPs by Light Microscopy:** Different concentrations of Ag NPs including 0.05, 0.1, 0.2, 0.3 and 0.4 mg/mL were prepared. To all concentrations, an amount of 100  $\mu$ l of protoscoleces was added. Subsequently, the test tubes were kept at 37°C for different times. The protoscoleces' viability was determined by 0.1% eosin. Also, the percentage of mortality was estimated by counting a minimum of 200 protoscoleces from each treatment. Hydatid fluid was considered a negative control, and 5% NaCl was positive. The experiments were repeated triplicate times (Shnawa *et al.*, 2017).

### *In vitro* Protoscolicidal Effect of Ag NPs by Scanning Electron Microscopy:

Ultrastructure examination with SEM was performed. Protoscoleces were immersed in pH 7.2 phosphate-buffered 2.5% glutaraldehyde for 24 h at 4°C for fixation. Serial incubations in ethanol (30, 50, 70, 90, and 100%) were done. Finally, they were dried and sputter-coated with a gold sputtering device (Desk Sputter Coater), and it was inspected by FESEM (Quanta 4500) SEM operating at 15 kV (Elissondo *et al.*, 2006; Shi *et al.*, 2016).

**Hemolysis test:** The hemolysis test of AgNPs was performed according to Huang *et al.* (2016) and Mesdaghinia *et al.* (2019). In brief, fresh blood was collected in a tube with EDTA. Amount of the diluted RBCs suspension was added to AgNP in PBS from different concentrations, include 0.05, 0.1, and 0.2, beside 0.3 mg/ml. RBCs suspensions were incubated at 37°C for one hour. Finally, the absorbance of the supernatants was estimated using UV-visible spectrophotometer at 570nm. Erythrocytes incubated in sterile PBS were considered a negative control. Another sample was treated with deionized distilled water, representing positive control. The following equation was used to calculate the percentage hemolysis of the erythrocytes.

Hemolysis percentage = [(specimens absorbance-negative control absorbance)/(positive control absorbance-negative control absorbance)]  $\times$  100 (Chen *et al.*, 2015; Oves *et al.*, 2018).

**Statistical analysis:** The results were analyzed by Graph pad Prism software version 8. The two-way ANOVA and Tukey's test were applied. A p-value less than 0.05 (<0.05) is statistically significant.

## RESULTS

Silver NPs were produced by leaves extract of *Z. spina - christi*. The visual inspection confirmed Ag Nanoparticles' formation by changing the mixture's color from greenish-yellow to dark brown.

The optical absorption of Ag NPs dispersed in water was recorded. Reduction of AgNO<sub>3</sub> to Ag was documented with UV-Vis instrument. The specimens exhibited UV absorption spectra with a peak at 460nm owing to surface plasmon resonance (Fig. 2A). During the

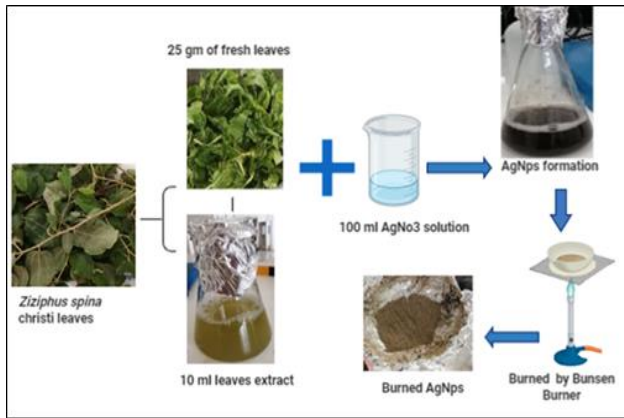


**Fig. 1:** A schematic illustration of the green synthesis of Silver Nanoparticles.

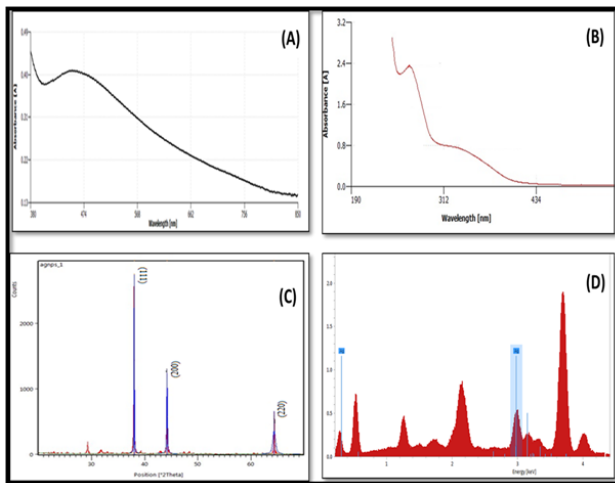


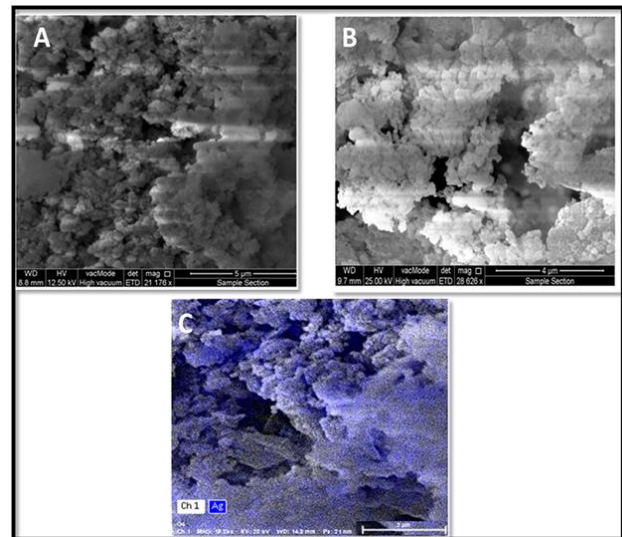
**Fig. 2:** A. The UV-Vis spectrum of synthesized Ag NPs using the extract of *Z. spina-christi*. B. The UV-Vis absorption spectrum from *Z. spina-christi* leaves extract. C shows the X-ray diffraction pattern from synthesized Ag NPs. D. illustrates the EDX spectrum synthesized Ag NPs.

biosynthesis of Ag NPs, changing the color of the mixture is the primary signal that appeared, confirming Ag NPs production.

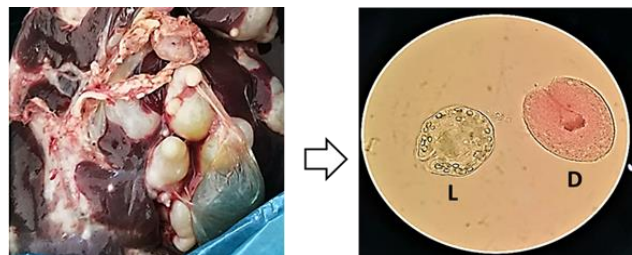
Regarding the results of the spectroscopic analysis of the *Z. spina-christi* extract, represented two signals at 320nm (the band I) and 266nm (bond II), are assigned to the cinnamoyl and benzoyl phenolic systems (Fig. 2B). These signals are linked to transitions from  $\pi$  to  $\pi^*$  that indicate phytochemicals from the leaf extraction. They would be a source for the green synthesis of metallic and metal oxide nanoparticles.

Fig. 2C shows the X-ray diffraction pattern from Ag NPs prepared by the green synthesized method; it approves the face-centered cubic structure. The dominant reflection peaks are 111, 200, and 220, corresponding with the scattering angles at 38.037°, 44.205°, and 64.344°, respectively. The resulted peaks equal with the JCPDS: No.36-1451, indicating the purity of the Ag NPs crystal.

Fig. 2D illustrates the EDX analysis of Ag NPs, which is formed using the bioreduction technique. It assured the existence of the Ag NPs. The other peaks besides Ag related to Au element in the EDX analysis resulted from using a gold coating to show better SEM images.



**Fig. 3:** A and B show the typical FE-SEM images of the Ag NPs synthesized using aqueous *Z. spina-christi* extract at different magnifications. The synthesized Ag NPs had spherical shapes, and the size of the particles was measured between 50 to 80 nm. C. The elemental mapping of the Ag NPs.



**Fig. 4:** Heavily infected liver of sheep. L, live protoscolex, and D dead protoscolex assessed by 0.1% eosin staining.

Fig. 3A and 3B present the typical FE-SEM images of the Ag NPs morphology at different magnifications. The identical distribution can be seen from the SEM micrographs. To some extent, Ag NPs are spherical-shaped, with some agglomerations of nanoparticles, and the average size was ranged between 50-80 nm. The elemental mapping analysis of the green synthesized metallic Ag NPs verified Ag Nanoparticles' constant presence on Ag Nanoparticles' surface, which indicates the creation of the Ag NPs (Fig. 3C).

**Viability of the Protoscoleces:** The protoscoleces were harvested from hydatid cysts of heavily infected sheep liver. Protoscoleces viability was assessed with eosin dye. Viable protoscoleces seemed to be colorless compared to dead ones that absorbed the stain and appeared red, the percentage of *in vitro* viability was 97% (Fig. 4), so it is appropriate for the subsequent experiments.

**Scolicidal Efficiency of Ag NPs:** The current study's findings indicated the powerful *in vitro* scolicidal efficacy of the biosynthesized Ag NPs. It showed that no viable protoscoleces was noticed after 2hr of incubation with Ag NPs at a 0.4 mg/ml concentration as in Fig. 5B. On the other hand, the control group's protoscoleces seemed colorless and viable during the experiment. They appeared to be morphologically intact with clear and bright calcareous corpuscles (Fig. 5A). The mortality within the

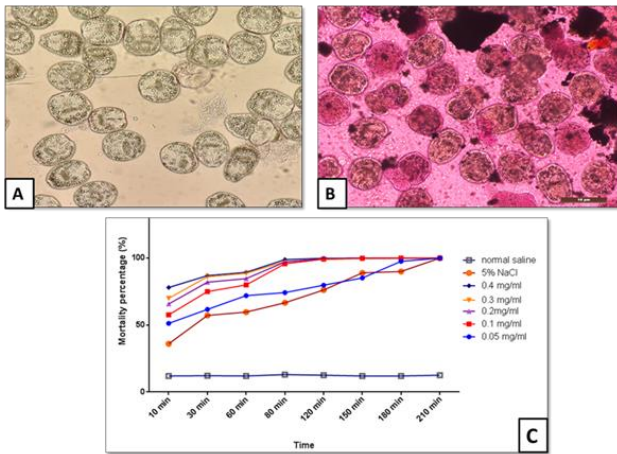


**Fig. 5:** A represents live untreated protoscolecoids of the control. B shows dead protoscolecoids after 2 hr. of incubation with Ag NPs at a 0.4 mg/ml concentration. C. *In vitro* protoscolicidal effect of Ag NPs at different incubation times.

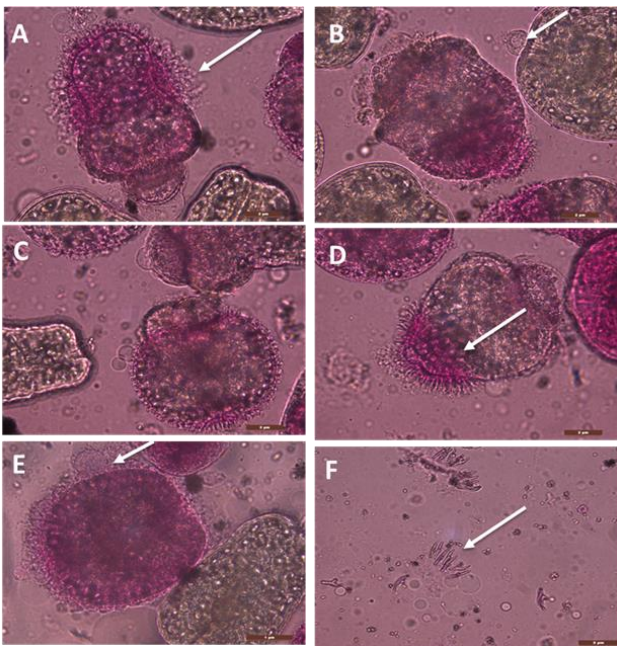


**Fig. 6:** Treated protoscolecoids with Ag NPs absorbed the Eosin stain. B, C & D illustrate protoscolecoids that partially absorbed the stain. A & E show the tegumental digitiform extensions at the outer tegument of protoscolecoids (arrow). F shows separated hooks and corpuscles.

protoscolecoids, which were incubated with different concentrations of Ag NPs compared to untreated control protoscolecoids, as illustrated in Fig. 5C. The highest protoscolicidal activity was recorded at 0.4 mg/ml, followed by 0.3 mg/ml, 0.2 mg/ml, 0.1 mg/ml, and 0.05 mg/ml. In contrast, the protoscolecoids of the control remain viable and seemed to be colorless. These outcomes indicated the dose-dependent activity of Ag NPs against protoscolecoids. The mortality percentages were increased with time in all concentrations of Ag NPs, which point out that the mortality percentage was also time-dependent.

**Morphological Effects of Ag NPs against *E. granulosus* Protoscolecoids:** The recent study revealed some protoscolecoids after incubation with Ag NPs absorbed the eosin dye, indicating their death (Fig. 6). Tegument of the parasite is the first part affected. Most of the protoscolecoids

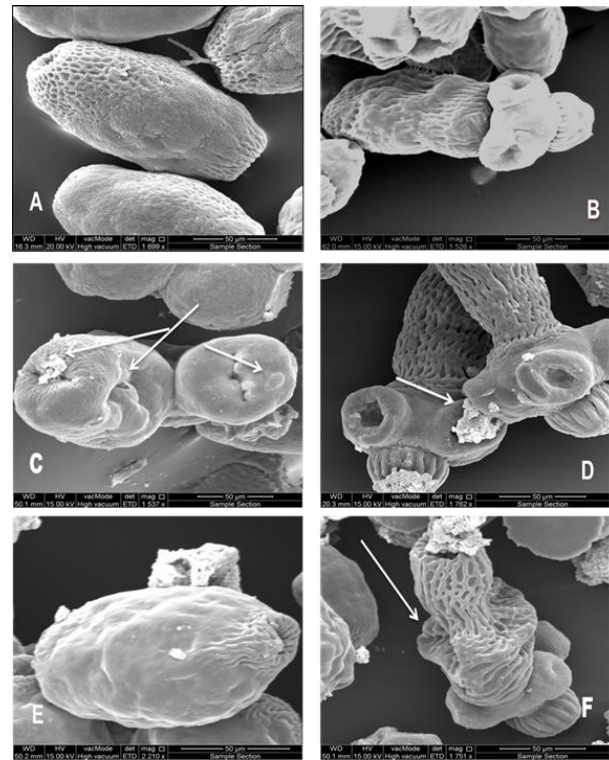


**Fig. 7:** A and B show normal control protoscolecoids. C treated protoscolecoids with Ag NPs show the presence of Ag NPs and the formation of a bleb. D, E, & F show different morphological changes, with the Ag NPs accumulation as white structures on the protoscolecoids.

were invaginated. They exhibited several alterations; include tegumental damage, disorganization of rostellar hooks, loss of calcareous corpuscles, and bleb appearance (Fig. 6B, C and E). Fig. 6A & E show the tegumental digitiform extensions at the outer tegument of protoscolecoids. Also, Fig. 6C and D show an evaginated protoscolecoids. They partially absorbed the eosin that indicates the initiation of their death, a group of separated hooks, as shown in Fig. 6F.

**The Ultrastructural Alteration of the Treated Protoscolecoids with Ag Nanoparticles:** To characterize the structural effects in the protoscolecoids induced by Ag NPs, they were prepared for SEM. No changes were detected in the ultrastructure of the protoscolecoids of the control group. They remained viable after 3hr of incubation during the experimental period (Fig. 7A and B). The outcomes of the viability experiment compatible with the destruction noticed at the ultrastructural examination. The prominent location of injury was the tegument of the protoscolecoids. At one hour after incubation, several blebs in the tegument of treated samples with 0.2 mg/ml were observed by SEM (Fig. 7C). These results confirmed the Ag NPs stimulate morphological destruction in the parasite. At half an hour post-incubation, symbols of ultrastructural modification were prominent: the soma part was shrunken. The evagination of protoscolecoid with rostellar distortion and disorganization was also detected (Fig. 7E and F).

Moreover, (Fig. 8A, B, C and D) illustrated the aggregation and the loss of the typical morphology of the treated protoscolecoids with the Ag NPs. Several protoscolecoids exhibited rostellar disorder, shedding of hooks and destruction of microtriches. Also, loss of hooks

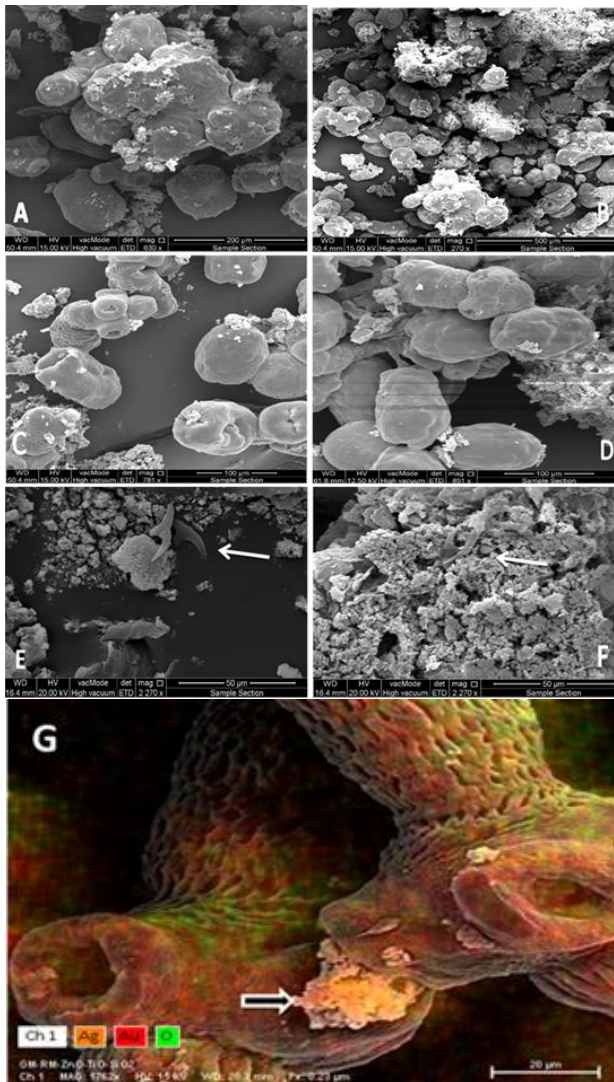


**Fig. 8:** Micrographs illustrate the ultrastructural damage of the treated protozoa with Ag NPs. A, B, C, and D show aggregation of distorted protozoa and the Ag NPs as white color. E and F illustrate the damaged protozoa with hooks (arrow). G, Corresponding mapping images of Ag NPs. Orange Nanoparticles' accumulation on two evaginated protozoa (arrow) with oxygen and gold as green and red.

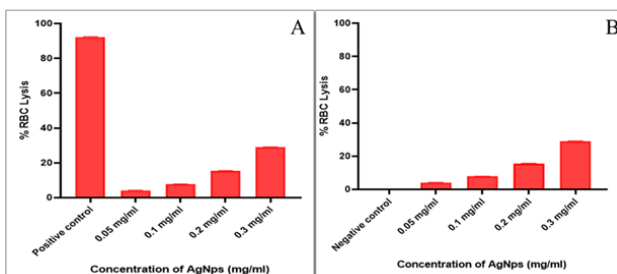


**Fig. 9:** Effect of different concentrations of Ag NPs on RBCs lysis compared to the positive (A) and negative controls (B).

has occurred, and it accumulated with the damaged parasite, as shown in Fig. 8 E and F. Finally, Fig. 8G shows two evaginated protozoa covered with Ag NPs, which appeared as orange color, while oxygen and gold expressed green and red color, respectively.

**Hemolysis test:** The biocompatibility of the synthesized Ag NPs was tested by performing RBCs lysis test. The

incubation of the Ag NPs with RBCs showed little toxicity and caused limited RBCs lysis. This lysis of RBCs at the doses of 0.05, 0.1, 0.2, and 0.3 mg/ml of AgNPs was detected as 4.2, 7.9, 15.6, and 29%, respectively, which were showed statistically significant decreases ( $P \leq 0.05$ ) compared with the positive control, thus proposing its biocompatibility. Nevertheless, with increasing concentration, erythrocytes viability was proportionally decreased (Fig. 9).

## DISCUSSION

Because of the medical applications, Nanoparticles of many metals, like, Au, Ag, Pt, and ZnO are widely tested. The green manufactured NPs are more stable, rapidly synthesized, and vastly diverse in morphology and size than those made by other organisms (Irvani, 2011). The biological synthesis of NPs has described a clean, non-toxic, and environmental-friendly technique compared to the other physical and chemical methods (Mittal *et al.*, 2013).

In the present study, silver NPs were produced using leaves extract of *Z. spina-christi*. The visual inspection proved the formation of Ag NPs. The color was changed from greenish-yellow to intense dark brown, confirming Ag NPs production. The presence of electron-rich functional groups in the plant is proposed to be accountable for Ag NPs formation. It is suggested that the plant materials serve as a reducing and stabilizing agent for Ag NPs production. The extracts' phytochemical composition was phenolic content, cardiac glycosides, polyphenols, saponins, and tannins (Abalaka *et al.*, 2010; Khaleel *et al.*, 2016; EL-Hefny *et al.*, 2018).

The UV-Vis spectroscopy technique is broadly performed for the structural categorization of NPs. The reduction of  $\text{AgNO}_3$  to Ag NPs is checked by double-beam UV-Vis spectrum. The samples showed UV absorption spectra with a peak at 460nm owing to the surface plasmon resonance (Fig. 1A). During the biosynthesis of Ag NPs, changing the color of the mixture is the primary signal that appears due to the surface plasmon resonance proving the release of Ag NPs. The obtained results of the Ag NPs had a perfect agreement with the previously reported literature. Arreche *et al.* (2018) described the silver nanoparticles as spherical, hexagonal, and triangular, with a particle size of 50nm. It presents a surface plasmon peak of about 460nm. The surface plasmon resonance band of Ag NPs was documented within a value between 452-465 nm in a study by Faried *et al.* (2016). Hassan *et al.* (2020) also observed the UV-Vis spectrum for AgNPs prepared using *Z. spina-christi* at 423-441 nm. The peak was amplified with increasing concentration of extract.

The present findings of EDX, X-ray diffraction and SEM imaging confirmed the green synthesis of Ag NPs by the plant extract.

Treatment of hydatid cyst disease is complex, and there are several methods worldwide. Including chemotherapy, surgical removal, watch and wait, and Percutaneous management of hepatic cyst with scolicidal material under ultrasound instrument or the Percutaneous-Aspiration-Injection Re-Aspiration or (PAIR) are considered as the primary management options (Giorgio *et al.*, 2009).

The superior method for hydatidosis treatment is surgery. However, leakage of hydatid fluid with protoscoleces during the operation is the significant cause of its secondary recurrence infection. Also, it may cause a fatal anaphylactic reaction (Ye *et al.*, 2016). Therefore, the injection of the cyst with protoscolicidal agents is an integral part of the surgery. Till now, there is no effective and safe agent. Consequently, new efficient scolical material with low side effects is highly recommended for urgent demand.

The current results demonstrated that the Ag NPs exhibited considerable protoscolicidal activity, which was time and dose-dependent. The maximum effect was observed at 0.4 mg/ml after 120 min of incubation as 100% mortality. This finding approximately complies with that of Norouzi *et al.* (2020), who found maximum scolical activity of Ag NPs was at 1 mg/mL after one hour of treatment, which expressed an 80% mortality percentage. Several alterations were detected in the protoscoleces' tegument exposed to Ag NPs that appeared dead as they absorbed the eosin stain.

The present findings agree with Xing *et al.* (2016), who revealed that the protoscoleces' tegument was the primary drug damage site. It exhibited several ultra-structural alterations when exposed to sodium arsenite within *in vitro*; this phenomenon may be attributed to stress responses. The cestodes' tegument is a cellular structure that has an essential role in the parasite's physiology. It is associated with nutrient absorption, protection from enzymatic and immunological effects of the host excretion, and ion exchange. Also, several essential enzymes are embedded in the protoscoleces tegument (McManus and Barret, 1985).

The alteration in the protoscoleces involved tegumental alteration, rostellar disorder, loss of rostellar hooks, the formation of several blebs on the tegument. The same finding was previously observed in the protoscoleces treated with different chemical substances such as flubendazole (Elissondo *et al.*, 2006) and thymol (Elissondo *et al.*, 2008). In this aspect, Pérez-Serrano *et al.* (1994) concluded that loss of hooks and appearance of blebs are "stress responses" that occurred in the parasite by exposure to a harmful environment. Furthermore, the tegument's alteration affects the tegumental microtrichea, which is perhaps related to parasite nutrition because microtrichea is related to nutrition absorption. The protoscoleces' death may be attributed to apoptosis or programmed cell death as a common reason for eukaryotic cell death.

Moreover, apoptosis has been recorded in hydatid cysts of *E. granulosus* Paredes *et al.*, 2007; Spotin *et al.*, 2012; Shi *et al.*, 2016). Also, Bakhtiar *et al.* (2020) proposed that apoptosis has a role in the host-*Echinococcus* metabolic interactions in suppressive and survival actions of cystic echinococcosis. The formation of digitiform projections on protoscoleces' tegument layer was documented in this study, leading to osmoregulatory damage into the parasite's tegumental layers. This osmoregulation impairment leads to the loss of turgidity due to leakage of cell contents, which might be the primary reason for the mortality in treated parasites (Verma *et al.*, 2014).

The results of the *in vitro* hemolytic ability of Ag NPs towards the human RBCs revealed that the percentage of hemolysis increased as the concentration of Ag NPs raised. However, it significantly differed from that of the positive control group. This proposition relies on the formation of AgCl by binding the Ag<sup>+</sup> ions with free chloride ions, reduced surface area owing to particle aggregation, and the appearance of a protein corona on particles. Therefore, the amount of unbound Ag<sup>+</sup> is limited in the Ag NPs -blood mixture that may destruct the erythrocytes. Moreover, direct particle interaction with the RBC membrane may also lead to hemolysis (Choi *et al.*, 2011). Also, RBCs' nonspecific uptake of nanoparticles was happened in an unclear mechanism according to particle size (just particles ≤200nm can enter the erythrocytes) (Rothen-Rutishauser *et al.*, 2006). The explanation for the hemolytic effect by Ag NPs proved in this work may be attributed to Ag<sup>+</sup> production, particle interaction with the RBCs, and particle uptake by the erythrocytes; nevertheless, the responsibility of each one is vague (Choi *et al.*, 2011). Nanoparticles can adsorb proteins to produce corona in the biological environment as a result of their high energy. Therefore, this altered surface affects its bioactivity and toxicity (Treuel *et al.*, 2015). Choi *et al.* (2011) pointed out that Ag NPs showed high hemolytic effect than Ag micron-sized ones, attributed to the large surface area, Ag<sup>+</sup> production, or the contact between the particles and the RBCs.

It has been mentioned that Ag nanoparticles express hemolysis via altering membrane integrity and surface features. Therefore, the erythrocyte's hemolysis is not just dependent on size. Osmotic lysis of the RBCs may result from the pore formed on its membrane by the NPS. Still, the real cause for erythrocyte membrane destruction is not identified. Moreover, reduced availability of Ag<sup>+</sup> could stimulate erythrocytes death *in vitro*, probably related to reactive oxygen species (Huang *et al.*, 2016).

**Conclusions:** Green synthesis of Ag NPs using *Z. spina-christi* leaves extracts was achieved in this work. This technique was environment friendly, non-toxic, cost-effective, and single-stepped. The synthesized Ag NPs were spherical and showed a characteristic UV-Vis absorption peak at 460 nm. XRD analysis also revealed the hexagonal wurtzite structure. The Ag NPs were characterized by EDS equipped with SEM, which confirmed the presence of NPs with an average size of 50-80 nm. The synthesized Ag NPs exhibited excellent efficiency as protoscolicidal agents.

*Z. spina-christi* could have a promising source of antioxidants for further pharmaceutical applications. Also, this paper investigated the hemolytic activity of Ag NPs as a model for cytotoxicity. The present findings showed no significant toxic effect of Ag NPs at low concentrations against RBCs. It may be emphasized that they are biocompatible for use as safe protoscolicidal agents at low doses.

**Authors contribution:** PJJ conducted the experiments, drew graphs, and wrote the draft of the manuscript. BHS and SMH designed and supervised the project and reviewed the article.

## REFERENCES

- Abalaka ME, Daniyan SY and Mann A, 2010. Evaluation of the antimicrobial activities of two *Ziziphus* species (*Ziziphus mauritiana* L. and *Ziziphus spina christi* L.) on some microbial pathogens. *Afr J Pharm Pharmacol*, 4:135-9.
- Arreche RA, Montes de Oca-Vásquez G, et al., 2018. Synthesis of Silver Nanoparticles Using Extracts from Yerba Mate (*Ilex paraguariensis*) Wastes. *Waste Biomass Valor* 11:245-53.
- Bakhtiar NM, Spotin A, Mahami-Oskouei M, et al., 2020. Recent advances on innate immune pathways related to host-parasite cross-talk in cystic and alveolar echinococcosis. *Parasit Vect* 13:232. <https://doi.org/10.1186/s13071-020-04103-4>.
- Barabadi H, Honary S, Ali Mohammadi M, et al., 2017. Green chemical synthesis of gold nanoparticles by using *Penicillium aculeatum* and their scolicidal activity against hydatid cyst protoscolices of *Echinococcus granulosus*. *Environ Sci Pollut Res Int* 24:5800-10. doi: 10.1007/s11356-016-8291-8.
- Benyan AK, Mahdi NK, Abdul-Amir F, et al., 2013. Second reported case of multilocular hydatid disease in Iraq. *Qatar Med J* 1:28-9.
- Chen LQ, Fang L and Ling J, 2015. Nanotoxicity of Silver Nanoparticles to Red Blood Cells: Size-Dependent Adsorption, Uptake, and Hemolytic Activity. *Chem Res Toxicol* 28:501-9.
- Choi J, Reipa V, Hitchins VM, et al., 2011. Physicochemical characterization and in vitro hemolysis evaluation of silver nanoparticles. *Toxicol Sci* 123:133-43.
- EL-Hefny M, Mohamed AA, Salem MZM, et al., 2018. Chemical composition, antioxidant capacity and antibacterial activity against some potato bacterial pathogens of fruit extracts from *Phytolacca dioica* and *Ziziphus spina-christi* grown in Egypt. *Scientia Horticulturae* 233:225-32.
- Elissondo M, Dopchiz M, Ceballos L, et al., 2006. In vitro effects of flubendazole on *Echinococcus granulosus* protoscolices. *Parasitol Res* 98:317-23.
- Elissondo MC, Albani CM, Gende L, et al., 2008. Eguaras M, Denegri G. Efficacy of thymol against *Echinococcus granulosus* protoscolices. *Parasitol Int* 57:185-90.
- Fariad M, Shamel K, Miyake M, et al., 2016. "A Green Approach for the Synthesis of Silver Nanoparticles Using Ultrasonic Radiation's Times in Sodium Alginate Media: Characterization and Antibacterial Evaluation. *J Nanomaterials* 11: <https://doi.org/10.1155/2016/4941231>.
- Giorgio A, Di Sarno A, de Stefano G, et al., 2009. Farella N, Matteucci P, Scognamiglio U, and Giorgio V, "Percutaneous Treatment of Hydatid Liver Cyst". *Recent Pat Antiinfect Drug Discov* 4:29.
- Halawani FEM, 2017. Rapid biosynthesis method and characterization of silver nanoparticles using *Ziziphus spina christi* leaf extract and their antibacterial efficacy in therapeutic application. *J B NB* 8:22-35.
- Hassan OM, Ibraheem IJ, Adil BH, et al., 2020. Synthesis of Silver Nanoparticles by ecofriendly environmental method using *Piper nigrum*, *Ziziphus spina-christi*, and *Eucalyptus globulus* extract. *J Physics: Conference Series* 1530:012139.
- Huang H, Lai W, Cui M, et al., 2016. An Evaluation of Blood Compatibility of Silver Nanoparticles. *Sci Rep* 6:25518. <https://doi.org/10.1038/srep25518>.
- Iravani S, 2011. Green synthesis of metal nanoparticles using plants. *Green Chem* 13:2638-50.
- Kern P, Menezes da Silva A, Akhan O, et al., 2017. The Echinococcoses: Diagnosis, clinical management, and burden of disease. *Adv Parasitol* 96:259-369.
- Khaleel SMJ, Jaran AS and Haddadin MSY, 2016. Evaluation of total phenolic content and antioxidant activity of three leaf extracts of *Ziziphus spina-christi* (Sedr) grown in Jordan. *J Adv Med Med Res* 14:1-8.
- McManus DP and Barrett NJ, 1985. Isolation, fractionation, and partial characterization of the tegumental surface from protoscolices of the hydatid organism, *Echinococcus granulosus*. *Parasitol* 90:111-29. doi:10.1017/s0031182000049064.
- Mesdaghinia A, Pourpak Z, Naddafi K, et al., 2019. An in vitro method to evaluate hemolysis of human red blood cells (RBCs) treated by airborne particulate matter (PM10). *MethodsX* 6:156-61.
- Mittal AK, Chisti Y and Banerjee UC, 2013. Synthesis of metallic nanoparticles using plant extracts. *Biotech Adv* 31:346-56. DOI: 10.1016/j.biotechadv.2013.01.003.
- Norouzi R, Ataie A, Hejazy M, et al., 2020. Scolicidal effects of nanoparticles against hydatid cyst protoscolices in vitro. *Int J Nanomedicine* 17:1095-100. <https://doi.org/10.2147/IJN.S228538>.
- Oluwaniyi OO, Adegoke HI, Adesuji ET, et al., 2016. Biosynthesis of silver nanoparticles using aqueous leaf extract of *Thevetia peruviana* Juss and its antimicrobial activities. *Appl Nanosci* 6:903-12.
- Oves M, Aslam M, Rauf MA, et al., 2018. Antimicrobial and anticancer activities of silver nanoparticles synthesized from the root hair extract of *Phoenix dactylifera*. *Mater Sci Eng C Mater Biol Appl* 1:429-43.
- Paredes R, Jiménez V, Cabrera G, et al., 2007. Apoptosis as a possible mechanism of infertility in *Echinococcus granulosus* hydatid cysts. *J Cell Biochem* 1;100(5):1200-9. doi: 10.1002/jcb.21108. PMID: 17031852.
- Pérez-Serrano J, Casado N, Guillermo, et al., 1994. The effects of albendazole and albendazole sulphoxide combination-therapy on *Echinococcus granulosus* in vitro. *Int J Parasitol* 24:219-24.
- Rahimi MT, Ahmadpour E, Rahimi Esboei B, et al., 2015. Scolicidal activity of biosynthesized silver nanoparticles against *Echinococcus granulosus* protoscolices. *Int J Surg*, 19: 128-33. <https://doi.org/10.1016/j.ijssu.2015.05.043>.
- Rothen-Rutishauser BM, Schürch S, Haenni B, et al., 2006. Interaction of fine particles and nanoparticles with red blood cells visualized with advanced microscopic techniques. *Environ Sci Technol* 40: 4353-9.
- Salih TA, Hassan KT, Majeed SR, et al., 2020. In vitro scolicidal activity of synthesised silver nanoparticles from aqueous plant extract against *Echinococcus granulosus*. *Biotechnol Rep* e00545. doi:10.1016/j.btre.2020.e00545.
- Shi H, Lei Y, Wang B, et al., 2016. Protoscolicidal effects of chenodeoxycholic acid on protoscolices of *Echinococcus granulosus*. *Exp Parasitol* 167:76-82.
- Shnawa BH, 2018. Advances in the use of Nanoparticles as anti-Cystic Echinococcosis agents: A Review Article. *J Pharm Res Int* 24:1-14.
- Shnawa BH, Gorony SHM and Khalid KM, 2017. Efficacy of *Cyperus rotundus* rhizomes tubers extracts against protoscolices of *Echinococcus granulosus*. *World J Pharm Res* 6:1-23.
- Siles-Lucas M, Casulli A, Cirilli R, et al., 2018. Progress in the pharmacological treatment of human cystic and alveolar echinococcosis: Compounds and therapeutic targets. *PLoS Negl Trop Dis* 12:e0006422 <https://doi.org/10.1371/journal.pntd.0006422>.
- Smyth J and Barrett N, 1980. Procedures for testing the viability of human hydatid cysts following surgical removal, especially after chemotherapy. *Trans R Soc Trop Med Hyg* 74:649-52.
- Spotin A, Majdi MM, Sankian M, et al., 2012. The study of apoptotic bifunctional effects in relationship between host and parasite in cystic echinococcosis: a new approach to suppression and survival of hydatid cyst. *Parasitol Res* 110:1979-84.
- Treuel L, Docter D, Maskos M, et al., 2015. Protein corona - from molecular adsorption to physiological complexity. *Beilstein J Nanotechnol* 6:857-73.
- Verma VC, Gangwar M and Nath G, 2014. Osmoregulatory and tegumental ultrastructural damages to protoscolices of hydatid cysts *Echinococcus granulosus* induced by fungal endophytes. *J Parasit Dis* 38:432-9.
- WHO, 2010. Working to overcome the global impact of neglected tropical diseases. First WHO report on neglected tropical diseases. Available:<http://www.who.int/iris/handle/10665/70503>.
- Xing G, Wang B, Lei Y, et al., 2016. In vitro effect of sodium arsenite on *Echinococcus granulosus* protoscolices. *Mol Biochem Parasitol* 207:49-55.
- Ye J, Zhang Q, Xuan Y, et al., 2016. Factors Associated with Echinococcosis-Induced Perioperative Anaphylactic Shock. *Korean J Parasitol* 54:769-75.